A simple, powerful diode laser system for atomic physics

ANDREW DAFFURN[1,*], RACHEL F. OFFER[2], AND AIDAN S. ARNOLD[1]

[1] Dept. of Physics, SUPA, University of Strathclyde, Glasgow, G4 0NG, UK,
[2] Institute for Photonics and Advanced Sensing (IPAS) and School of Physical Sciences, University of Adelaide, Adelaide, SA 5005, Australia
[*] andrew.daffurn@strath.ac.uk

Compiled July 7, 2021

External-cavity diode lasers are ubiquitous in atomic physics and a wide variety of other scientific disciplines, due to their excellent affordability, coherence length and versatility. However, for higher power applications, the combination of seed lasers, injection-locking and amplifiers can rapidly become expensive and complex. Here we present a high-power, single-diode laser design with specifications: $>210\,\mathrm{mW}$, $100\,\mathrm{ms}$-linewidth $(427 \pm 7)\,\mathrm{kHz}$, >99% mode purity, $10\,\mathrm{GHz}$ mode-hop-free tuning range and $12\,\mathrm{nm}$ coarse tuning. Simple methods are outlined to determine the spectral purity and linewidth with minimal additional infrastructure. The laser has sufficient power to collect 10^{10} ^{87}Rb atoms in a single-chamber vapour-loaded magneto-optical trap. With appropriate diodes and feedback, the system could be easily adapted to other atomic species and diode laser architectures. © 2021 Optical Society of America

http://dx.doi.org/10.1364/ao.XX.XXXXXX

1. INTRODUCTION

The invention of the laser [1] was a landmark moment for the scientific world and the ability to generate monochromatic, coherent light has opened avenues for research in many fields including atomic physics [2], telecommunications [3, 4], and measurement science [5, 6]. Its use in atomic physics precipitated the fields of laser spectroscopy [7, 8] and laser cooling, which have led to applications in frequency and timing metrology [9–11], magnetometry [12, 13] and inertial sensing [14–17].

External-cavity diode lasers (ECDLs) are a popular choice for these purposes [18–22] and they can be constructed by operating a semiconductor diode in conjunction with optical feedback provided by a diffraction grating. The diode's sensitivity to feedback tempers the undesirable spectral properties of the device [23], narrowing the linewidth by orders of magnitude (also by feedback-free routes [24]). This generally results in a device with high tunability and narrow linewidth at a reasonable cost. The atomic or molecular species and transition of interest determines the choice of components, particularly the laser diode and grating, however a wide range of wavelengths are accessible from home-made ECDLs for assisting laser cooling of K at 405 nm [25] or Sr at 497 nm [26], to compact ECDLs for water vapor absorption at 1.4 µm [27].

The ever-growing power demands and complexity of atomic physics experiments have resulted in the development of various solutions to fulfil a multitude of requirements. Where great stability and reliability are required this can be achieved with, e.g.: lasers using interference-filter based feedback [28, 29]; modular laser systems demonstrating month-long sub-MHz locking [30]; micro-integrated ECDLs with no movable parts for harsh, challenging space-based environments [31]; and distributed bragg reflector (DBR [32]) or distributed feedback (DFB [33]) laser systems.

For applications requiring considerable power, one can conveniently pass a few mW of power from a narrow linewidth seed diode laser system through a tapered amplifier (TA), preserving the seed linewidth but with output power of order 1 W [34, 35]. Due to poor mode quality typically around half the TA power is lost in fibre coupling [36]. Commercial TAs can cost tens of thousands of pounds, although bespoke 'home-made' systems can be made by skilled users for a fraction of the cost, albeit with more assembly time.

High-power alternatives include frequency-doubling telecommunications wavelength light in a nonlinear crystal or waveguide [37] and sum-frequency mixing. Ti:Sapphire laser systems [38] have additional benefits in terms of linewidth and intensity stability, however there is a concomitant increase in cost into the £100k range.

Here, we present an intermediate system that retains the low cost, narrow linewidth advantage of typical ECDLs, but uses a newly available 300 mW high-power diode to bridge the power gap to TAs. Our design reduces the financial barrier for developing $\gtrsim$100 mW experiments, a power range that is routinely required for alkali atom laser cooling systems. Most alkali metal atoms have stretched-state transition [39] saturation intensities of order $\approx 1\,\mathrm{mW/cm^2}$. For single-beam intensities

beyond this saturation intensity atom number also saturates, and hence the 210 mW output power we achieve is already sufficient to saturate e.g. a single-cell vapour-loaded ^{87}Rb magneto-optical trap with 10^9 [40] to 10^{10} [16] atoms using total powers of $20-200$ mW split into three orthogonal pairs of $2.5-5.0$ cm diameter retro-reflected beams.

Our findings support the idea that modern medium power commercial diodes, using architectures like quantum well and ridge waveguide, still function well in ECDL setups. In addition, we characterise the spectral purity and linewidth of our high power ECDL using simple methods which require minimal additional diagnostic equipment.

2. ECDL

Traditional double heterostructure laser diodes used in ECDLs are limited to output powers of 10s of milliWatts. However, more complicated diode architectures are now available for relatively low cost. The diode [41] in our high power ECDL uses a combined quantum well and ridge waveguide structure, which allows 300 mW output power to be reached at a typical central wavelength of 785 nm.

To test this new diode we retrofitted it to a pre-existing Littrow configuration ECDL. The device is based on an inexpensive and easily manufactured design [20], which includes only simple modifications to commercially available components. More information on the design and electronics are available in Appendix A and D of Ref. [40], and we note minor subsequent changes in a footnote [42]. Feedback is provided by an 1800 lines mm^{-1} visible reflective holographic grating [43]. This produces 11.4 % feedback at operational wavelengths with the light polarised parallel to the lines of the grating, balancing wavelength selectivity with output power. Higher output powers should be achieved using gold-coated $(+15\%)$ and/or UV $(+12\%)$ gratings, although the latter will reduce feedback.

With the high power diode installed, the ECDL achieves a 780 nm output power of 210 mW off the grating, before roll-off starts to occur at input currents of 350 mA. We measure a diode lasing threshold of around 75 mA, and have demonstrated 70% efficiency coupling to single mode fibre, indicating high spatial mode purity compared to a typical tapered amplifier.

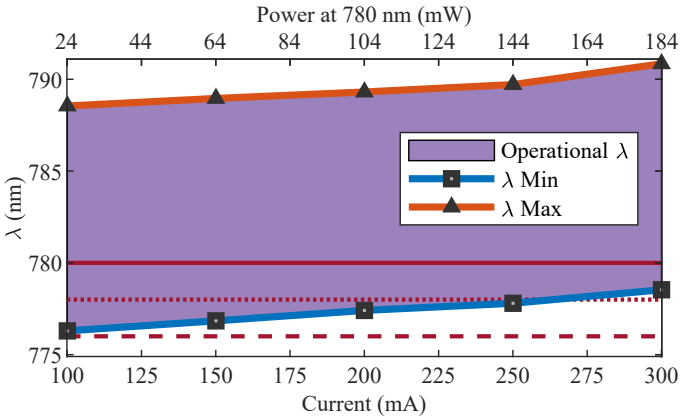

Fig. 1. Wavelength tuning range of the ECDL at 14 °C. Also shown are the 780 nm (solid line), 776 nm (dashed line), and 2-photon 778 nm (dotted line) wavelengths, representing transitions in Rb. Note that, in suitably designed systems, extreme temperatures can dramatically extend the tuning range [44].

The diode was cooled with a 33 W thermoelectric Peltier (TEC) to around 14 °C. At this temperature it is always possible to address the D_2 Rb lines at 780 nm at the operating currents for the device (Fig. 1). In humid environments with high dew point temperatures [45], this represents the device's operational limit without compromising diode longevity, but the Rb 2-photon 778 nm transition is already accessible (Fig. 1), and diode wavelength tuning is $\approx 0.3\,\mathrm{nm}/^{\circ}\mathrm{C}$. By engineering the laser environment [44] dramatic temperature changes can vary available laser wavelengths by 10s of nanometres.

3. MODE-HOP-FREE RANGE

Ideally, a laser operates in a single resonator mode, which arises from the interplay between the semiconductor material, cavity length, external cavity, and feedback. An important characteristic is the mode-hop-free tuning of the device, this represents the maximum continuous frequency range the laser can scan before there is a modal jump. The material and cavity length are properties of the diode, and external feedback can be fine-tuned by altering the horizontal and vertical angle of the grating with respect to the diode. A short cavity is desirable to maximise the mode-hop-free scan range. However, a shorter cavity length has the effect of increasing the laser's linewidth. The external cavity length selected here of approximately 20 mm allows for both a useful continuous scan range and narrow linewidth.

For our device the mode-hop-free range was at least 10 GHz, making it possible to continuously scan across all Doppler-broadened D_2 lines of ^{87}Rb and ^{85}Rb (Fig. 2). This was achieved by adjusting the external cavity spacing using a piezo-electric transducer (PZT) and simultaneously scanning the current via a feed-forward signal [46]. For this particular diode, scanning via the PZT alone yields a mode-hope-free range of only 2 GHz.

4. AMPLIFIED SPONTANEOUS EMISSION

We are also interested in the percentage of coherent light produced by the laser, i.e. light from stimulated emission. Amplified spontaneous emission (ASE) that is reflected in the diode optical cavity produces lasing at threshold. However, an excess of ASE limits the maximum gain in the material and contaminates the laser beam with a broad-spectrum incoherent background.

The mode purity of the light can be measured using an optical spectrum analyser, but these devices are expensive and generally have low resolution so are unable to spectrally resolve signals at the MHz scale of the laser linewidth. A Fabry-Perot etalon can also be used, but this again necessitates additional equipment which requires careful alignment. We demonstrate an easy technique that simply requires a vapour cell – which would already be required as part of a lab setup for locking the laser to an atomic line.

To measure the ASE of our device hyperfine pumping spectroscopy [47], widely misleadingly known as 'saturated absorption spectroscopy', was performed on a heated Rb cell. Heating the cell dramatically increases the Rb atom number density in the cell, with an additional relatively minor effect on the width $(\propto \sqrt{T})$ of the Doppler-broadened absorption features [48–50]. For a completely coherent laser in a well-heated cell 100 % of the light would be absorbed at these Doppler broadened features, and any remaining light is a product of ASE. From Fig. 2 the remaining broadband ASE light that is transmitted through the cell is around 1 %, matching what we have seen from other lower power 780 nm laser diode systems.

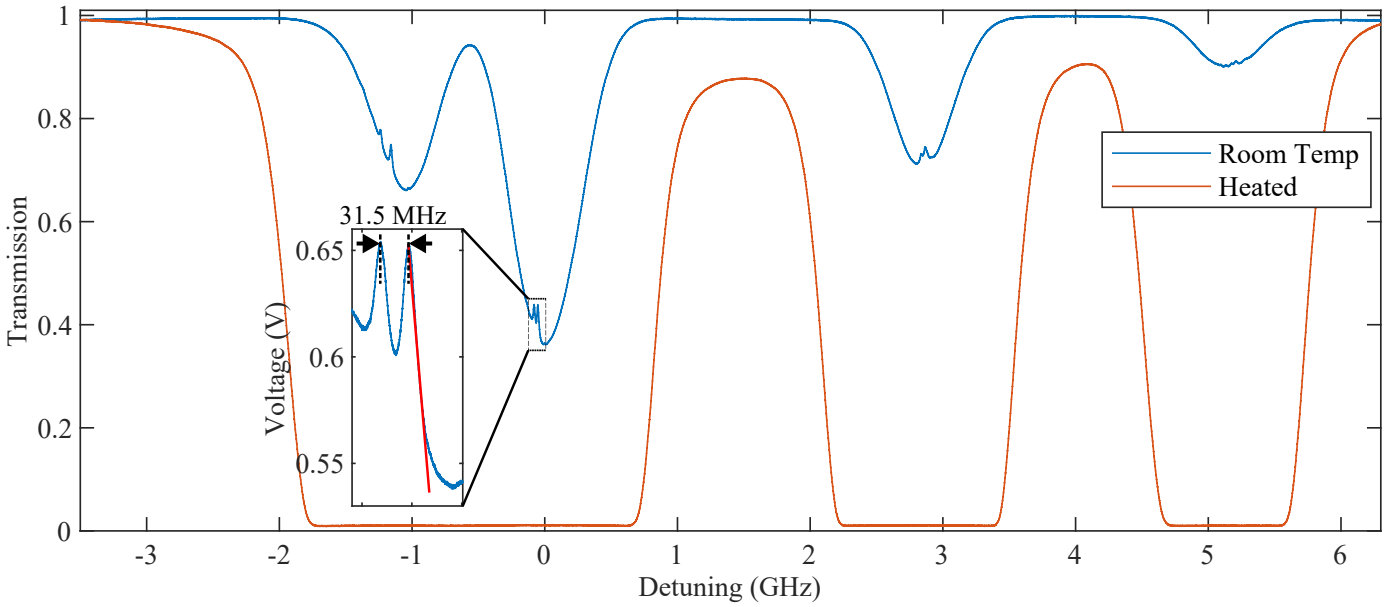

Fig. 2. Single-trace hyperfine pumping spectra of the Rb D_2 line at room temperature (blue) and in a heated cell (orange) with input beam intensity of 17 mW cm^{-2}. The normalised photodiode absorption data have been adjusted to remove a $-0.0083\,\mathrm{GHz}^{-1}$ gradient introduced by the feed-forward scan. Inset: ^{85}Rb $F = 3 \rightarrow F' = 3, 4$ crossover transition peak with red line to highlight slope where the free-running laser is 'parked' for the linewidth measurement.

5. LINEWIDTH

Finally, we demonstrate a quick and easy method to measure the linewidth of a laser. A standard technique is to measure a radio frequency (RF) beat note, using a fast photodiode and an RF spectrum analyser [51, 52]. However, a beat note requires at least two lasers (two technically only suffice if the laser linewidth to be measured is much larger than the reference laser). Alternatively a beat note can also be measured using a self-heterodyning method [53], but this requires a sufficiently long length of fibre for a given linewidth. The method described here only requires a vapour cell hyperfine pumping spectroscopy setup, which is already required for a sub-Doppler atomic lock.

We measure the linewidth by using a high resolution feature in the photodiode absorption spectrum as a frequency discriminator [54]. The peak selected was the ^{85}Rb D_2 $5S_{1/2}$ $F = 3 \rightarrow 5P_{3/2}$ $F' = 2, 3$ crossover transition (Fig. 2 inset), because of the relatively large and linear peak slope (red line with magnitude of slope 6.3 mV MHz^{-1}), however in principle any peak could be selected. The calibration trace is recorded first, then the free-running laser is frequency-tuned to the side of the crossover pumping peak (red slope, Fig. 2 inset) and the transmitted power fluctuations are recorded for 1 s at 1 MS/s on an oscilloscope, yielding inferred laser frequency vs. time. This method yielded a root-mean-square (RMS) linewidth of (427 ± 7) kHz for an averaging time of 100 ms, with an indicative standard error from 10 traces. A separate commercial diode laser had a free-running linewidth of 510 kHz using the same technique.

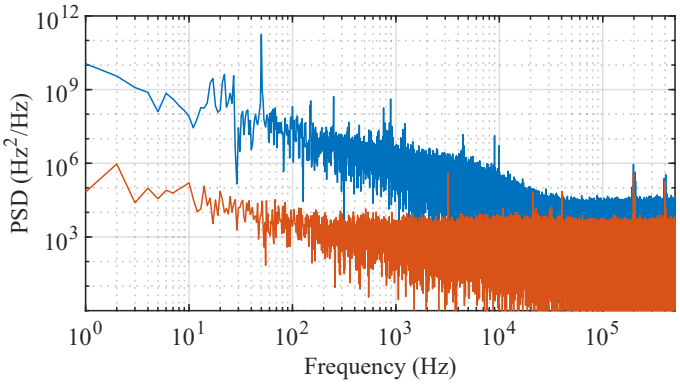

Fig. 3. Power spectral density from analysis of the noise data. Laser noise (blue) and background intensity noise (red). Analysis of the laser noise led to a 100 ms linewidth of (427 ± 7) kHz.

The resulting power spectral density of one 1 s linewidth measurement is also displayed in Fig. 3. The upper frequency end of the noise spectrum will be limited by the photodiode roll-off frequency of 8kHz [55]. Note the observed linewidth is nonetheless likely to be an upper estimate, as the 50 Hz mains peak contributes to half the linewidth, and we have also not added the complexity of detecting (and subsequently removing) the contribution from laser intensity noise.

To evaluate the accuracy of these linewidth measurements, we compared to a standard beat-note measurement technique, however a beat-note typically yields relative power as a function of frequency. The time-dependent photodiode traces from the two lasers were therefore also converted to histograms of relative power vs. laser frequency, to enable an approximate comparison to the beat-note. The histograms were approximately normally distributed, with Gaussian fits yielding RMS linewidths for the home-built and commercial lasers of 490 kHz and 530 kHz, respectively, similar to the raw RMS values above. This gave a combined linewidth of 720 kHz when the two linewidths were added in quadrature. This value can be compared favourably to the 700 kHz RF beat note RMS linewidth of the two lasers from

a spectrum analyser, using a Gaussian fit to the beat note over the same 100 ms averaging time.

Additionally, this method can be used to evaluate the time-dependence of the linewidth [52]. A 1 s noise measurement can be split into smaller samples and used to evaluate the RMS linewidths for varying averaging times, a figure illustrating the linewidth's time-dependence is included as part of the dataset [56].

6. CONCLUSION

We have developed an economical home-build ECDL solution that can produce hundreds of mW of continuous power with a free-running 100 ms linewidth of (427 ± 7) kHz. It is a single-unit, inexpensive source of moderate power for atomic physics experiments involving rubidium and is currently operating as one of the pump lasers in a four-wave mixing experiment [57, 58]. We have also detailed cost- and time-effective techniques to determine various useful laser characteristics, including the spectral purity and linewidth.

For applications requiring sub-kHz linewidths, the laser system could also work in conjunction with an appropriate high-finesse cavity lock [59, 60].

Funding. Funding via the Leverhulme Trust (Grant No. RPG-2013-386) and EPSRC (Grant No. EP/M506643/1).

Acknowledgments. In addition to the support provided by the funding organisations, we are grateful for valuable discussions with Jonathan Pritchard and Erling Riis.

Disclosures. The authors declare no conflicts of interest.

Data availability. Data underlying the results presented in this paper are available in Ref. [56].

REFERENCES

1. T. Maiman, "Stimulated Optical Radiation in Ruby," Nature **187**, 493 (1960).
2. C. E. Wieman and L. Hollberg, "Using diode lasers for atomic physics," Rev. Sci. Instrum. **62**, 1–20 (1991).
3. G. Gibson, J. Courtial, M. J. Padgett, M. Vasnetsov, V. Pastextquotesingleko, S. M. Barnett, and S. Franke-Arnold, "Free-space information transfer using light beams carrying orbital angular momentum," Opt. Express **12**, 5448 (2004).
4. H. J. Kimble, "The quantum internet," Nature **453**, 1023–1030 (2008).
5. A. D. Ludlow, M. M. Boyd, J. Ye, E. Peik, and P. O. Schmidt, "Optical atomic clocks," Rev. Mod. Phys. **87**, 637–701 (2015).
6. R. Elvin, G. W. Hoth, M. Wright, B. Lewis, J. P. McGilligan, A. S. Arnold, P. F. Griffin, and E. Riis, "Cold-atom clock based on a diffractive optic," Opt. Express **27**, 38359 (2019).
7. P. Micke, T. Leopold, S. A. King, E. Benkler, L. J. Spieß, L. Schmöger, M. Schwarz, J. R. C. López-Urrutia, and P. O. Schmidt, "Coherent laser spectroscopy of highly charged ions using quantum logic," Nature **578**, 60–65 (2020).
8. F. S. Ponciano-Ojeda, F. D. Logue, and I. G. Hughes, "Absorption spectroscopy and Stokes polarimetry in a $^{87\$}$Rb vapour in the Voigt geometry with a 1.5 T external magnetic field," J. Phys. B **54**, 015401 (2021).
9. W. F. McGrew, X. Zhang, R. J. Fasano, S. A. Schäffer, K. Beloy, D. Nicolodi, R. C. Brown, N. Hinkley, G. Milani, M. Schioppo, T. H. Yoon, and A. D. Ludlow, "Atomic clock performance enabling geodesy below the centimetre level," Nature **564**, 87 (2018).
10. K. J. Arnold, R. Kaewuam, A. Roy, T. R. Tan, and M. D. Barrett, "Blackbody radiation shift assessment for a lutetium ion clock," Nat. Commun. **9**, 1650 (2018).
11. M. Takamoto, I. Ushijima, N. Ohmae, T. Yahagi, K. Kokado, H. Shinkai, and H. Katori, "Test of general relativity by a pair of transportable optical lattice clocks," Nat. Photonics **14**, 411–415 (2020).
12. D. Budker and M. Romalis, "Optical magnetometry," NP **3**, 227–234 (2007).
13. S. J. Ingleby, C. O'Dwyer, P. F. Griffin, A. S. Arnold, and E. Riis, "Vector Magnetometry Exploiting Phase-Geometry Effects in a Double-Resonance Alignment Magnetometer," Phys. Rev. Appl. **10**, 034035 (2018).
14. I. Dutta, D. Savoie, B. Fang, B. Venon, C. h. e. G. Alzar, R. Geiger, and A. Landragin, "Continuous Cold-Atom Inertial Sensor with 1 nrad/s Rotation Stability," Phys. Rev. Lett. **116**, 183003 (2016).
15. Y. Bidel, N. Zahzam, C. Blanchard, A. Bonnin, M. Cadoret, A. Bresson, D. Rouxel, and M. Lequentrec-Lalancette, "Absolute marine gravimetry with matter-wave interferometry," Nat. Commun. **9**, 627 (2018).
16. Y. Zhai, C. H. Carson, V. A. Henderson, P. F. Griffin, E. Riis, and A. S. Arnold, "Talbot-enhanced, maximum-visibility imaging of condensate interference," Optica **5**, 80 (2018).
17. C. Overstreet, P. Asenbaum, T. Kovachy, R. Notermans, J. M. Hogan, and M. A. Kasevich, "Effective Inertial Frame in an Atom Interferometric Test of the Equivalence Principle," Phys. Rev. Lett. **120**, 183604 (2018).
18. K. B. MacAdam, A. Steinbach, and C. Wieman, "A narrow-band tunable diode laser system with grating feedback, and a saturated absorption spectrometer for Cs and Rb," Am. J. Phys. **60**, 1098–1111 (1992).
19. L. Ricci, M. Weidemüller, T. Esslinger, A. Hemmerich, C. Zimmermann, V. Vuletic, W. König, and T. Hänsch, "A compact grating-stabilized diode laser system for atomic physics," Opt. Commun. **117**, 541–549 (1995).
20. A. S. Arnold, J. S. Wilson, and M. G. Boshier, "A simple extended-cavity diode laser," Rev. Sci. Instrum. **69**, 1236–1239 (1998).
21. E. C. Cook, P. J. Martin, T. L. Brown-Heft, J. C. Garman, and D. A. Steck, "High passive-stability diode-laser design for use in atomic-physics experiments," Rev. Sci. Instrum. **83**, 043101 (2012).
22. E. Brekke, T. Bennett, H. Rook, and E. L. Hazlett, "3D printing an external-cavity diode laser housing," Am. J. Phys. **88**, 1170–1174 (2020).
23. R. Lang and K. Kobayashi, "External optical feedback effects on semiconductor injection laser properties," IEEE J. Quantum Electron. **16**, 347–355 (1980).
24. P. D. McDowall and M. F. Andersen, "Acousto-optic modulator based frequency stabilized diode laser system for atom trapping," Rev. Sci. Instrum. **80**, 053101 (2009).
25. G. Unnikrishnan, M. Gröbner, and H.-C. Nägerl, "Sub-Doppler laser cooling of ^{39}K via the 4S→5P transition," SciPost Phys. **6**, 047 (2019).
26. V. Schkolnik, O. Fartmann, and M. Krutzik, "An extended-cavity diode laser at 497 nm for laser cooling and trapping of neutral strontium," Laser Phys. **29**, 035802 (2019).
27. A. Jiménez, T. Milde, N. Staacke, C. Aßmann, G. Carpintero, and J. Sacher, "Narrow-line external cavity diode laser micro-packaging in the NIR and MIR spectral range," Appl. Phys. B **123**, 207 (2017).
28. X. Baillard, A. Gauguet, S. Bize, P. Lemonde, P. Laurent, A. Clairon, and P. Rosenbusch, "Interference-filter-stabilized external-cavity diode lasers," Opt. Commun. **266**, 609–613 (2006).
29. D. J. Thompson and R. E. Scholten, "Narrow linewidth tunable external cavity diode laser using wide bandwidth filter," Rev. Sci. Instrum. **83**, 023107 (2012).
30. D. Sahagun, V. Bolpasi, and W. von Klitzing, "A simple and highly reliable laser system with microwave generated repumping light for cold atom experiments," Opt. Commun. **290**, 110–114 (2013).
31. E. Luvsandamdin, S. Spießberger, M. Schiemangk, A. Sahm, G. Mura, A. Wicht, A. Peters, G. Erbert, and G. Tränkle, "Development of narrow linewidth, micro-integrated extended cavity diode lasers for quantum optics experiments in space," Appl. Phys. B **111**, 255–260 (2013).
32. J. M. Pino, B. Luey, S. Bickman, and M. H. Anderson, "Miniature, compact laser system for ultracold atom sensors," in *Photonic Applications for Aerospace, Commercial, and Harsh Environments IV,* A. A. Kazemi, B. C. Kress, and S. Thibault, eds. (SPIE, 2013).
33. E. D. Gaetano, S. Watson, E. McBrearty, M. Sorel, and D. J. Paul, "Sub-megahertz linewidth 780.24 nm distributed feedback laser for ^{87}Rb

applications," Opt. Lett. **45**, 3529 (2020).
34. R. A. Nyman, G. Varoquaux, B. Villier, D. Sacchet, F. Moron, Y. Le Coq, A. Aspect, and P. Bouyer, "Tapered-amplified antireflection-coated laser diodes for potassium and rubidium atomic-physics experiments," Rev. Sci. Instrum. **77**, 033105 (2006).
35. J. C. B. Kangara, A. J. Hachtel, M. C. Gillette, J. T. Barkeloo, E. R. Clements, S. Bali, B. E. Unks, N. A. Proite, D. D. Yavuz, P. J. Martin, J. J. Thorn, and D. A. Steck, "Design and construction of cost-effective tapered amplifier systems for laser cooling and trapping experiments," Am. J. Phys. **82**, 805–817 (2014).
36. D. Voigt, E. Schilder, R. Spreeuw, and H. van Linden van den Heuvell, "Characterization of a high-power tapered semiconductor amplifier system," Appl Phys B **72**, 279–284 (2001).
37. S. S. Sané, S. Bennetts, J. E. Debs, C. C. N. Kuhn, G. D. McDonald, P. A. Altin, J. D. Close, and N. P. Robins, "11 W narrow linewidth laser source at 780nm for laser cooling and manipulation of Rubidium," Opt. Express **20**, 8915 (2012).
38. C. S. Adams, E. Riis, A. I. Ferguson, and W. R. C. Rowley, "Precision measurement of the $2\,^3S \rightarrow 3\,^3P$ transition in ^{4}He," Phys. Rev. A **45**, R2667–R2670 (1992).
39. From ground $nS_{\frac{1}{2}}|F = I + \frac{1}{2}\rangle$ to excited $nP_{\frac{3}{2}}|F' = I + \frac{3}{2}\rangle$ states using $m_F = \pm(I + \frac{1}{2}) \rightarrow m_{F'} = \pm(I + \frac{3}{2})$, for nuclear spin I.
40. A. S. Arnold, "Preparation and manipulation of an ^{87}Rb Bose-Einstein condensate," Thesis, University of Sussex (1999).
41. Thorlabs LD785-SH300.
42. The piezo-electric transducer (PZT) is replaced with a (safer!) low-voltage stack in a sapphire/brass housing under a mirror-mount actuator, allowing PZT frequency scan directly using standard $\pm 15\,\mathrm{V}$ analogue locking circuits, with the $-15\,\mathrm{V}$ output connected to the (electrically isolated) PZT 'ground' lead. A useful modification to the lock electronics is to include a digital switch allowing a controllable disconnection between the integrator and lock-in. Due to the low free-running laser linewidth, this allows the laser to be unlocked, jumped to other frequencies, jumped back, and relocked for excursions up to $\sim 1\,\mathrm{s}$. Note the ICL8038 signal generator chip is obsolete, but alternatives exist.
43. Thorlabs GH13-18V.
44. W. G. Tobias, J. S. Rosenberg, N. R. Hutzler, and K.-K. Ni, "A low-temperature external cavity diode laser for broad wavelength tuning," Rev. Sci. Instrum. **87**, 113104 (2016).
45. Like Glasgow.
46. S. C. Doret, "Simple, low-noise piezo driver with feed-forward for broad tuning of external cavity diode lasers," Rev. Sci. Instrums **89**, 023102 (2018).
47. D. A. Smith and I. G. Hughes, "The role of hyperfine pumping in multilevel systems exhibiting saturated absorption," Am. J. Phys. **72**, 631–637 (2004).
48. P. Siddons, C. S. Adams, C. Ge, and I. G. Hughes, "Absolute absorption on rubidium D lines: comparison between theory and experiment," J. Phys. B **41**, 155004 (2008).
49. M. A. Zentile, J. Keaveney, L. Weller, D. J. Whiting, C. S. Adams, and I. G. Hughes, "ElecSus: A program to calculate the electric susceptibility of an atomic ensemble," Comp. Phys. Commun. **189**, 162–174 (2015).
50. J. Keaveney, C. S. Adams, and I. G. Hughes, "ElecSus: Extension to arbitrary geometry magneto-optics," Comp. Phys. Commun. **224**, 311–324 (2018).
51. L. Turner, K. Weber, C. Hawthorn, and R. Scholten, "Frequency noise characterisation of narrow linewidth diode lasers," Opt. Commun. **201**, 391–397 (2002).
52. N. V. Bandel, M. Myara, M. Sellahi, T. Souici, R. Dardaillon, and P. Signoret, "Time-dependent laser linewidth: beat-note digital acquisition and numerical analysis," Opt. Express **24**, 27961–27978 (2016).
53. H. Ludvigsen, M. Tossavainen, and M. Kaivola, "Laser linewidth measurements using self-homodyne detection with short delay," Opt. Commun. **155**, 180–186 (1998).
54. A. Willis, A. Ferguson, and D. Kane, "Longitudinal mode noise conversion by atomic vapour," Opt. Commun. **122**, 31–34 (1995).
55. The roll-off frequency is limited by the $2\,\mathrm{m}$ RG58 coaxial cable to the oscilloscope, with estimated capacitance $165\,\mathrm{pF}$ and a response time of $\approx 20\,\mu\mathrm{s}$ in parallel with the $100\,\mathrm{k}\Omega$ resistor of the photodiode circuit.
56. Dataset DOI: 10.15129/53bc86dd-e859-4eac-824c-0273d4667989 (2021).
57. R. F. Offer, D. Stulga, E. Riis, S. Franke-Arnold, and A. S. Arnold, "Spiral bandwidth of four-wave mixing in Rb vapour," Commun. Phys. **1**, 84 (2018).
58. R. F. Offer, A. Daffurn, E. Riis, P. F. Griffin, A. S. Arnold, and S. Franke-Arnold, "Gouy phase-matched angular and radial mode conversion in four-wave mixing," Phys. Rev. A **103**, L021502 (2021).
59. R. Legaie, C. J. Picken, and J. D. Pritchard, "Sub-kilohertz excitation lasers for quantum information processing with Rydberg atoms," J. Opt. Soc. Am. B **35**, 892 (2018).
60. P. H. Moriya, Y. Singh, K. Bongs, and J. E. Hastie, "Sub-kHz-linewidth VECSELs for cold atom experiments," Opt. Express **28**, 15943 (2020).